Differences in electron depth-dose curves calculated with EGS and ETRAN and improved energy-range relationships

D. W. O. Rogers and A. F. Bielajew
Division of Physics, National Research Council of Canada, Ottawa, Ontario K1A 0R6, Canada

(Received 7 February 1986; accepted for publication 30 May 1986)

For 1–50 MeV electrons incident on a water phantom there are systematic differences in the depth-dose curves calculated by the Monte Carlo codes EGS and ETRAN (and its descendants SANDYL, CYLTRAN, ACCEPT, and the ITS system). Compared to ETRAN, the EGS code calculates a higher surface dose and a slightly slower dose falloff past the dose maximum. The discrepancy in the surface dose is shown to exist because the modified Landau energy-loss straggling distribution used in ETRAN underestimates the mean energy loss by about 10% since it underestimates the number of large energy-loss events. Comparison to experimental data shows a preference for the EGS depth-dose curves at 10 and 20 MeV. Since various dosimetry protocols assign electron beam energies based on measured depth-dose curves in water, formulas based on these more accurate EGS4 calculations are presented: (i) relating the mean energy of an incident electron beam to R_{50}, the depth at which the dose in a water phantom falls to 50% of its maximum value; and (ii) relating the most probable energy of the incident beam to the projected range of the depth-dose curve. A study is presented of the effects of the incident electron spectrum on the calculated depth-dose curve.

I. INTRODUCTION

The ETRAN code was developed at the National Bureau of Standards (U.S.) by Berger and Seltzer for doing Monte Carlo calculations involving coupled electron–photon radiation transport.[1–4] This code (actually, a long series of codes) has been tested against a wide variety of experimental data.[4–6] Results calculated with ETRAN have been extensively used in national protocols for clinical dosimetry such as those of the AAPM[7] and NACP,[8] in the report of the ICRU on electron dosimetry,[9] and in the ICRP's recommendations on radiation safety limits.[10] For these reasons, ETRAN is the code against which many major coupled electron–photon Monte Carlo systems have been benchmarked. However, the EGS code system[11,12] is known to differ from ETRAN in its calculated depth-dose curves for broad beams of electrons incident on a water phantom.[13] The purpose of this paper is to elucidate the differences, to explain them, and to compare the predictions of both codes with some experimental data. We will show that the EGS code more accurately simulates reality for electron depth-dose curves in the 1–50 MeV energy range.

Figure 1 compares the depth-dose curves for broad beams of 20-MeV electrons on water as calculated by EGS, ETRAN, and CYLTRAN.[14] Compared to EGS, ETRAN calculates a lower dose near the surface, a comparable peak dose, and a more rapid falloff to a similar practical range. This is typical for incident energies from below 1 MeV to over 50 MeV. The CYLTRAN results (done at NRCC) and the ETRAN results (done by Berger and Seltzer[3]) are practically identical, as they should be since they are essentially the same code. At the same time the EGS results agree within the statistical uncertainties of about 1% with the Monte Carlo results of Nahum[15] (see Fig. 7 of Ref. 13) and Andreo.[16,17]

Although the calculations presented in Fig. 1 were ostensibly done using the same stopping powers, we have verified that differences in stopping powers did not cause the discrepancies observed. Figure 2 presents EGS4 calculations using three different electron stopping powers for the same broad parallel beam of 20-MeV electrons on water. Although there are variations in the calculated depth-dose curves, they are much smaller than the observed EGS versus ETRAN differences.

As we will show below, the difference near the surface arises because the energy-loss straggling distribution which is used by ETRAN[1] (based on the Blunck–Leisegang modification of the Landau theory) does not give the correct mean energy loss.[16,22–24] We shall demonstrate this by some explicit calculations which are described in the next section, and then show that the experimental data for electron depth-

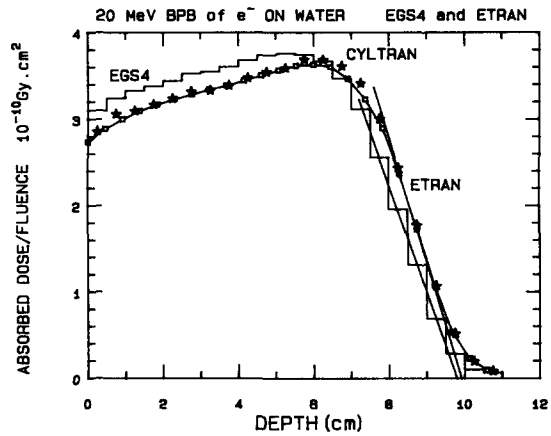

FIG. 1. Depth-dose curves for broad parallel beams of 20-MeV electrons incident on a slab of water as calculated by EGS4 (histogram), CYLTRAN (stars), and ETRAN (smooth curve with boxes). All curves were calculated with the 1964 stopping powers (Ref. 18). The straight lines show the similarity of the calculated practical ranges. For the EGS4 calculations, AE = ECUT = 0.700 MeV, ESTEPE = 4%. For the CYLTRAN calculations, ECUT = 0.7 MeV (total energy).

 0094-2405/86/050687-08$01.20

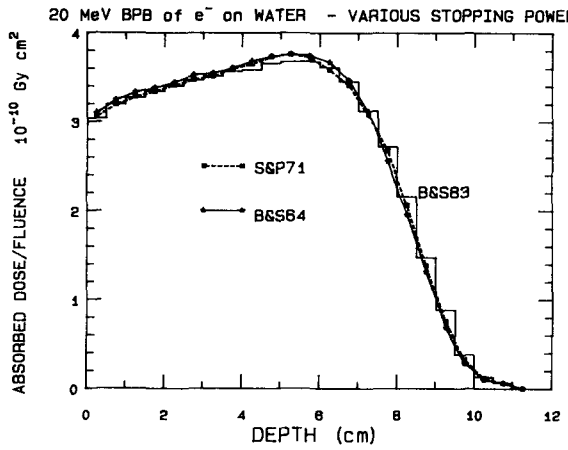

FIG. 2. Depth-dose curves for broad parallel beams of 20-MeV electrons incident on water as calculated using EGS4 and a variety of stopping powers. The histogram was calculated using the 1983 Berger and Seltzer stopping powers (Ref. 19) ($I = 75$ eV, density effect δ from Ref. 20); the dashed curve was calculated using $I = 75$ eV and δ from the general formula of Steinheimer and Peierls (Ref. 21); the line with stars was calculated using the 1964 stopping powers of Berger and Seltzer (Ref. 18) ($I = 65$ eV, δ identical to Berger and Seltzer).

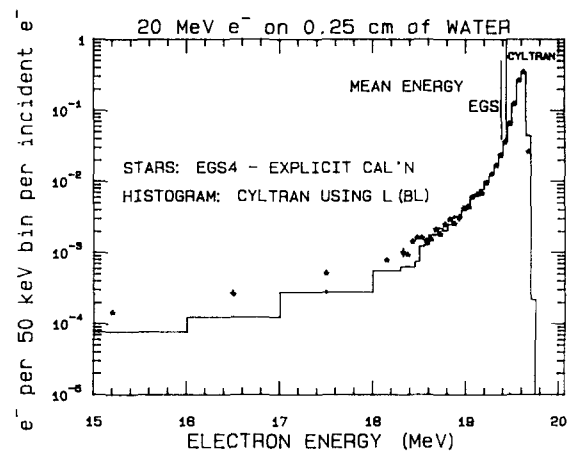

FIG. 3. Energy-loss straggling distribution of primary electrons for a beam of 20-MeV electrons passing through a 0.25-cm-thick slab of water. The EGS4 results (stars) were calculated by explicitly taking into account the creation of all secondary electrons with energies above 1 keV. The CYLTRAN results (histogram) were calculated by sampling from the Landau energy-loss distribution as modified by Blunck and Leisegang [L(BL)]. There is excellent agreement in the shape above 18.5 MeV but the underestimate of the large energy-loss events by the L(BL) distribution leads to a 9% underestimate of the mean energy loss compared to the EGS calculation and the total stopping-power estimate (see Table I).

dose curves show a preference for the EGS calculations in which the correct mean energy loss is used. We present a formula relating the most probable energy of the electron beam incident on the phantom surface to the projected range. We conclude by discussing the relationship between the mean electron energy at the surface of the phantom and the depth at which the dose falls to 50% of the maximum dose. The AAPM dosimetry protocol, using values based on the ETRAN calculations, has used this parameter to specify an electron beam's energy.

II. ENERGY-LOSS STRAGGLING IN EGS AND ETRAN

EGS and ETRAN treat energy-loss straggling in fundamentally different ways. Energy-loss straggling comes from the statistical fluctuations in the energy lost in events which create bremsstrahlung photons or secondary (knock-on) electrons. The EGS code takes this straggling into account explicitly by decreasing the energy of an electron each time it creates a knock-on electron above a threshold called AE or a bremsstrahlung photon above a threshold called AP. It has been shown that by using sufficiently small values of AE and AP, a realistic distribution of energy losses can be achieved.[25] However, in many situations it is primarily the energy-loss straggling induced by creating high-energy knock-on electrons or high-energy bremsstrahlung photons which affects the quantity being calculated and accurate results can be obtained with quite high values of AE and AP.[25,26]

In contrast, ETRAN and its descendants (such as SANDYL,[27] CYLTRAN,[14] ACCEPT,[28] and the ITS series[29]) sample the collisional energy loss in each electron step from the Landau distribution as modified by Blunck and Leisegang[1,4] [we will call this the L(BL) distribution]. There is no explicit correlation between the creation of a secondary electron and the energy of the primary electron. Energy loss due to the creation of secondary electrons is only taken into account in a statistical sense through the L(BL) distribution. The problem is that the L(BL) distribution does not predict the correct mean energy loss.[16,22-24,30] The mean energy loss predicted by the L(BL) distribution is about 10% less than that predicted by the corresponding electron collision stopping power. However, ETRAN accounts for energy-loss straggling due to the creation of bremsstrahlung photons by decreasing the electron's energy in the same manner as EGS.

Figure 3 presents a comparison of the distribution of energies of primary electrons after a 20-MeV beam passes through a 0.25-cm slab of water as calculated by EGS and CYLTRAN (which we take here and elsewhere to be the same as ETRAN). These distributions include the effects of collisional and radiative energy losses. This comparison is similar to one published previously,[25] except that here only primary electrons are considered to draw attention to the differences in the mean energy loss. Primary electrons emerging from the water slab with energies much below 10 MeV must have created a bremsstrahlung photon since an electron cannot give up more than half its energy in creating a secondary electron. The EGS and CYLTRAN results are in excellent agreement below 10 MeV, as expected, since they handle bremsstrahlung emission in similar ways. We conclude that the differences shown in Fig. 3 are due entirely to the problems with the collisional energy-loss straggling in CYLTRAN.

Table I presents the mean energy losses for 20-MeV electrons passing through a 0.25-cm water slab calculated in a variety of ways. It is clear that the L(BL) energy-loss distribution used in CYLTRAN (ETRAN) underestimates the mean energy loss by 9%, whereas the EGS code is in good agreement with the expected value. [Here and elsewhere we ignore the fact that the calculated energy losses include the radiative as well as collisional losses (see also footnote c to

TABLE I. Mean energy lost by 20-MeV electrons passing through a 0.25-cm slab of water.[a]

	Mean energy loss (keV)
EGS	613
ETRAN–CYLTRAN	
including straggle	562
no straggling	612
1964 stopping power	618[b]

[a] The slab is sufficiently thin that angular deflections are negligible. Calculations with both the Monte Carlo codes use the 1964 Berger and Seltzer stopping powers (Ref. 18).

[b] The Monte Carlo calculations include energy losses from radiative as well as collisional events which contribute 102 and 516 keV, respectively, to the energy loss calculated from the stopping powers.

Table II)]. The CYLTRAN result is also in good agreement if the energy-loss straggling is switched off. In the EGS calculation, 96.2% of the electrons have energies above 18.5 MeV and these electrons have an average energy of 19.529 MeV, whereas with CYLTRAN (ETRAN), 97.9% of the electrons are above 18.5 MeV and have the same average energy, viz., 19.533 MeV. Thus one sees that the L(BL) energy-loss distribution and the explicit Monte Carlo calculation of the energy loss are in good agreement for the distribution of energy losses less than 1.5 MeV, but the L(BL) distribution underestimates the number of large energy-loss events and this results in an underestimate of the mean energy loss by 9%. This should not be surprising since the L(BL) theory explicitly assumes that energy losses are small.[1] However, the small but important errors in the calculated number of events with a large energy loss appear to be more related to numerical accuracy of fitting functions rather than a breakdown in this assumption.[24,38]

The differences in the spectral shapes in Fig. 3 occur in regions where the number of electrons per MeV has fallen to less than 0.3% of the peak value. These differences would be almost impossible to detect experimentally. This explains why comparisons of the ETRAN code to experimental data for electrons passing through foils have not identified this problem.

In a thick phantom, the surface dose is primarily governed by the collisional stopping power of the incident electrons except for the effects of the transport of secondary electrons. Thus this underestimate of the mean energy loss explains the 9% lower surface dose calculated with ETRAN as opposed to EGS, since both codes handle secondary electron transport in roughly the same manner.

We found that the L(BL) formalism as implemented in CYLTRAN (and presumably ETRAN) underestimates the mean energy loss in thin slabs of water by about 10% for all electron energies between 1 and 50 MeV (see Table II). This explains why these differences occur for the depth-dose curves throughout the entire energy region studied.

III. PRACTICAL RANGE AND OTHER CONSIDERATIONS

Figure 4 presents a comparison of the continuous slowing down approximation (CSDA) range, the practical ranges computed using the formulas given by Berger and Seltzer[3] and by the ICRU[9] (their Eq. 3.21 which is the same as that given by the NACP[8]) and those ranges extracted from the depth-dose curves calculated with EGS4. In all cases except the ICRU formula, the 1983 stopping powers have been used.[19] The EGS data is reproduced over the energy range 3–50 MeV to within 0.5% by

$$E_p = 0.29 + 1.940\,R_p + 0.00684\,R_p^2, \quad (1)$$

where R_p is the practical range in cm extrapolated to the bremsstrahlung background, and E_p is in MeV. Up to 20 MeV there is remarkably good agreement between the EGS4 and ETRAN results, although by 50 MeV there is a 6% difference. Given the 10% difference in the mean energy loss

TABLE II. Mean energy lost by primary electrons passing through a slab of water with a thickness of $1/40 \times r_0$, the CSDA range for electrons in water, as calculated using the total stopping power or using the CYLTRAN Monte Carlo code which uses the L(BL) formalism for collisional energy loss.

		Energy lost passing through foil		
E_e (MeV)	$1/40\,r_0$ (cm)	CYLTRAN[a] (keV)	Stopping power[b] (keV)	Difference (%)
1	0.0109	18.5	20.6	−10.3
5	0.0638	114.5	128.5	−10.9
10	0.124	243	271	−10.3
20	0.233	520	576	−10.0
50	0.496	1510	1620	−7.0[c]

[a] Mean energy lost by primaries as calculated by CYLTRAN.

[b] Energy loss calculated using Berger and Seltzer (1964) stopping powers (Ref. 18).

[c] This value appears lower because the radiative energy loss is becoming significant and is (presumably) done correctly by CYLTRAN. Assuming the difference is entirely due to collisional energy-loss problems, the difference would be 10.7% for the collisional events.

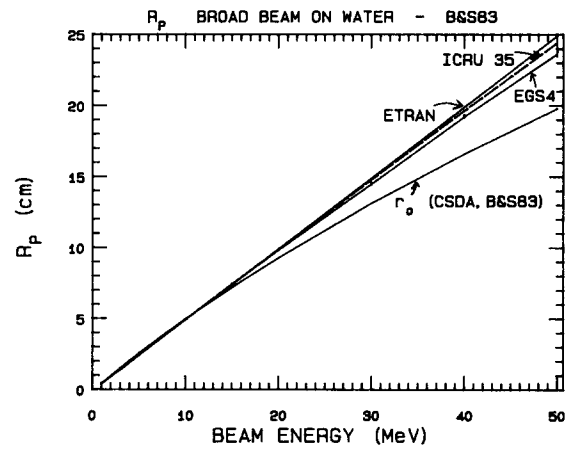

FIG. 4. A comparison of the practical ranges (above the bremsstrahlung tail) R_p, as calculated with EGS4 and ETRAN using the 1983 stopping powers (Ref. 19) and as calculated with the empirical formula recommended by ICRU-35 (Eq. 3.21 of Ref. 9) and the Nordic protocol (Ref. 8). The corresponding CSDA range r_0, calculated with the same stopping powers, is also shown.

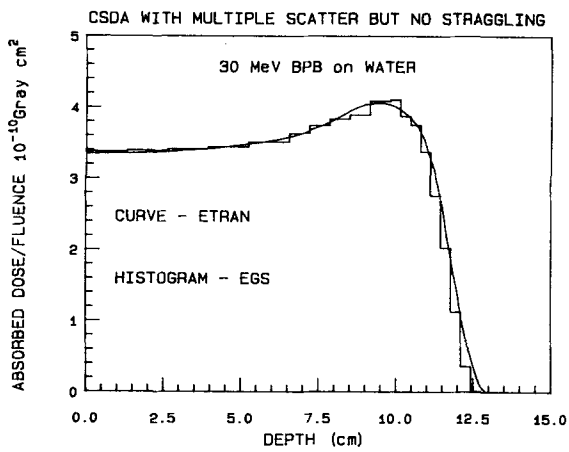

FIG. 5. Comparison of depth-dose curves for broad beams of 30-MeV electrons incident on a water phantom as calculated by EGS4 and ETRAN (Ref. 2) with no energy-loss straggling and with secondary electron and bremsstrahlung photon processes treated in the CSDA. The similarity of these curves shows that differences in the Molière and Goudsmit–Saunderson multiple scattering theories used by EGS and ETRAN, respectively, do not cause significant differences in the depth-dose curves. Including energy-loss straggling reduces the surface dose in the ETRAN calculations by roughly 10%, but does not change the EGS surface dose.

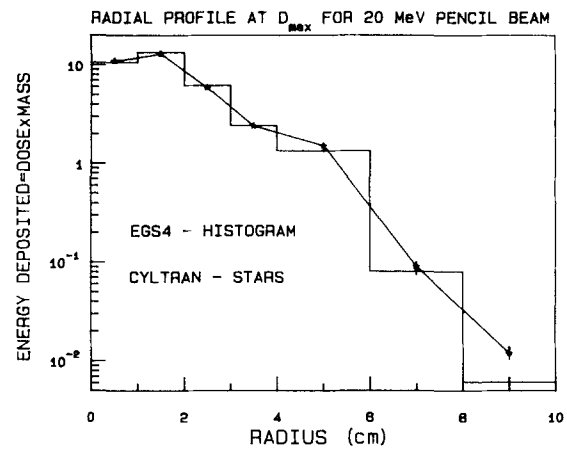

FIG. 6. Radial profile of the energy deposited in a water phantom by a 20-MeV pencil beam of electrons at a depth corresponding to D_{max} ($Z = 0.6$–$0.7\ r_0$) in a broad beam as calculated by EGS4 (histogram) and CYLTRAN. Note that this is a log plot and the height of each bin corresponds to the total energy deposited in this bin. The small differences in the bins at large radii seem unlikely to be indicative of a significant difference. The calculations have not been normalized but correspond to the same total dose within 1% for a broad beam. Note that for these EGS pencil beam calculations it was found necessary to use a step size with ESTEPE = 1%, whereas the broad beam results are insensitive to step size.

calculated by each code, the good agreement below 20 MeV seems somewhat surprising. However, as pointed out by Nahum (personal communication), it can be understood by recalling from Fig. 3 that the differences between the energy-loss straggling distributions occur only for those electrons suffering large energy losses. Those electrons reaching the practical range of the beam are just those electrons which have undergone no large energy-loss events. Thus one expects the two codes to predict similar practical ranges since they treat the small energy-loss events virtually identically (see Fig. 3). At energies above 20 MeV, the practical range calculated by EGS4 begins to differ from those calculated by ETRAN. Presumably, this is because even those electrons reaching the practical range have undergone some large energy-loss events. Since ETRAN underestimates these, it is not surprising that it predicts a slightly longer practical range.

EGS and ETRAN use the Moliere and Goudsmit–Saunderson multiple scattering formalisms, respectively. To date there have been no significant differences found between the results calculated with these two formalisms for low-Z materials (see, e.g., Berger[1] and Rogers[25]). Figure 5 presents a comparison of broad beam depth-dose curves calculated with EGS and ETRAN when energy-loss straggling and secondary electron transport have been turned off. It is clear that if there are any differences in the multiple scattering they will make at most small differences in the calculated depth-dose curves, although they may partially explain the differences in R_p.

Another difference between the two codes is that EGS takes into account the correlation between the creation of a knock-on electron and the primaries' angle and energy, whereas ETRAN does not. This implies forward going electrons have a slightly higher energy in EGS than in ETRAN. Figure 6 shows the radial energy deposition profiles at the depth corresponding to the peak dose in a broad beam but for a 20-MeV pencil beam as calculated by EGS4 and ETRAN. There is only a very small difference between the results of the two codes. The comparison between ETRAN and experiment presented by Lax, Brahme, and Andreo[31] shows that the radial distribution calculated by ETRAN is somewhat too broad. This suggests the EGS4 results are in better agreement with experiment since they are somewhat less broad. However, these are small differences and are not expected to affect the overall depth-dose curves.

IV. COMPARISON TO EXPERIMENT

Comparison to experimental data is the ultimate test of any calculation. However, completely specified experimental data are hard to come by. Shortt *et al.*[32] have presented some benchmark data for 10- and 20-MeV electron beams incident on a water phantom with and without small air and aluminium inhomogeneities embedded in it. In that paper, the most probable beam energies were determined from the measured practical range and mean energies inferred from Monte Carlo calculations of the difference between the most probable and mean energies. Subsequent studies have independently calibrated the beam energy and have shown agreement to within 0.1 MeV (Ross and Shortt[33]).

In Figs. 7 and 8 we present a comparison of the experimental central axis depth-dose data for beams with mean energies of 19.84 and 9.93 MeV compared to the results calculated with EGS4 and ETRAN for point sources of 20- and 10-MeV electrons passing through 100 cm of vacuum. The experimental data are arbitrarily normalized to the two calculations which are both absolute. While the agreement between the calculations and experiment is not perfect, there is a clear preference for the EGS calculations compared to the ETRAN (CYLTRAN) results. The experimental data are higher near the surface and fall off more slowly than

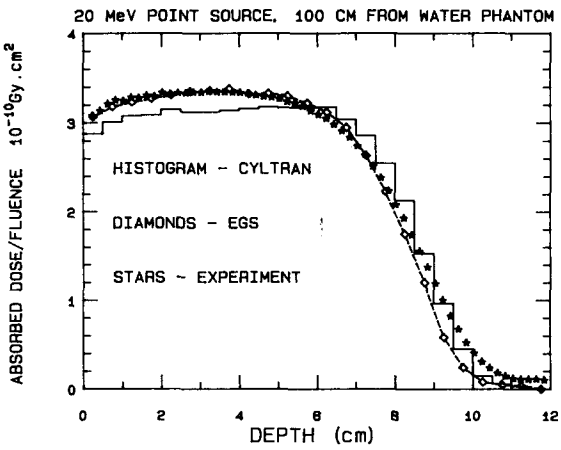

FIG. 7. Comparison of a measured central axis depth-dose curve in water (Ref. 32) (stars) with those calculated using EGS or CYLTRAN (ETRAN) for a point source of monoenergetic 20-MeV electrons, 100 cm in vacuum from the phantom surface. The mean and most probable energies of the experimental data were estimated to be 19.84 and 20.49 MeV, respectively.

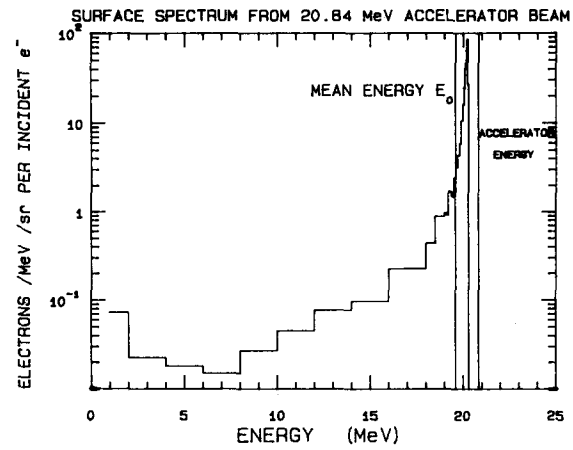

FIG. 9. The calculated electron number spectrum (including secondaries) near the central axis at the water surface after a monoenergetic pencil beam of 20.84-MeV electrons passes through the Ti exit window, Pb scattering foil, air, and Styrofoam in the beam's path.

EGS, whereas ETRAN is lower near the surface and falls off more quickly than EGS. Previous experimental results at 20 MeV have been summarized by Andreo and Brahme.[16] Their data are consistent with the current results, although they have renormalized their depth axis to give identical practical ranges for all cases.

We have done several auxiliary calculations to try to explain the differences between the EGS results and the experimental data. The use of a monoenergetic beam of electrons with the nearly correct mean energy has meant that various features (most notably, the practical range) are incorrect. To investigate these effects further, we modeled the experiment as a monoenergetic beam of electrons passing through the 0.0127-cm Ti exit window of the accelerator, the 0.0127-cm Pb scattering foil, 102 cm of air, and 3.9 cm of Styrofoam. We scored the electron number spectra near the central axis of the beam as they entered the water phantom. These calculated spectra are shown in Figs. 9 and 10. The point of showing these spectra (which do not include any effects of the accelerator energy spread) is to show that the mean energies of the spectra are significantly influenced by the very small low-energy tails. This means that experimental verification with a spectrometer would be difficult. Furthermore, it implies that one would also expect small but significant differences if these spectra were calculated with ETRAN because of the problems discussed above concerning large energy-loss events in the L(BL) distribution.

In Figs. 11 and 12 we present the depth-dose curves calculated for incident broad parallel beams with three different spectra, viz., with the full spectrum and with monoenergetic beams with energies equal to the most probable (E_p) and mean ($\overline{E}_0$) electron energies in the incident full spectrum. Several interesting points emerge. Firstly, note that R_{50}, the depth to 50% of maximum dose, is not the same for the calculations with the full spectrum and those with the monoenergetic $\overline{E}_0$ incident spectrum. This is because the low-energy tail plays a role in defining $\overline{E}_0$ and suggests that, contrary to common practice,[7,9] R_{50} does not provide an ideal specification of $\overline{E}_0$. In these cases, R_{50} varied by 0.8% (10 MeV) and 1.7% (20 MeV) for two spectra with the same value of

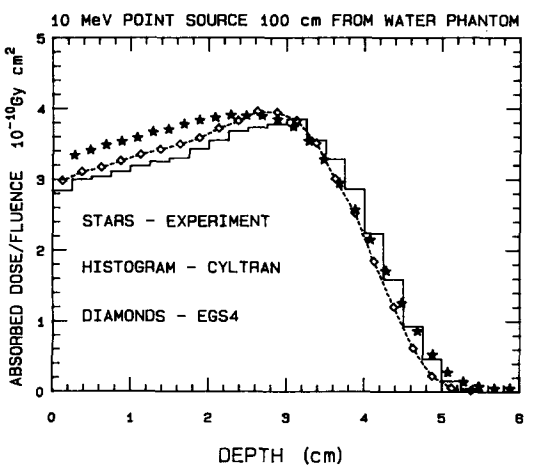

FIG. 8. As in Fig. 7 but for a monoenergetic 10-MeV point source simulating an experimental beam with $E_0 = 9.93$ MeV and $E_p = 10.11$ MeV (Ref. 32).

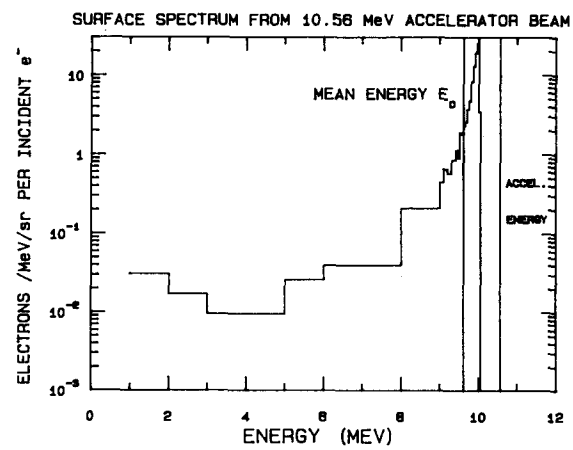

FIG. 10. As in Fig. 9 but for an incident 10.56-MeV beam.

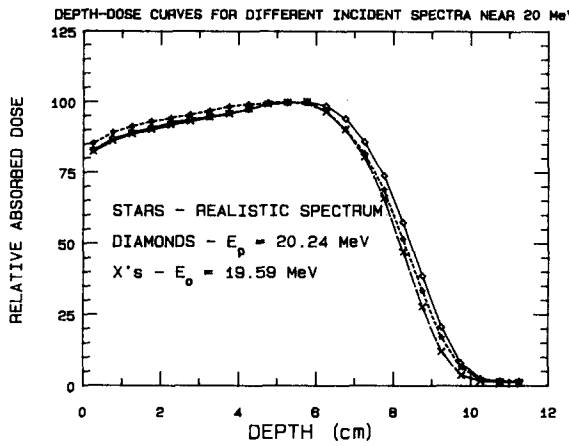

FIG. 11. Comparison of depth-dose curves calculated with EGS4 for broad parallel beams with different incident spectra. The realistic spectrum is that shown in Fig. 9 and the other two monoenergetic spectra correspond to E_p and E_0 for that spectrum. These calculations are for comparison only and do not correspond to the experimental data in Fig. 7 (default ESTEPE used).

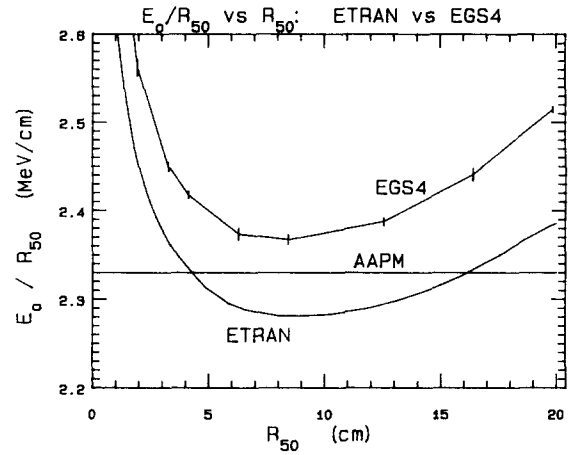

FIG. 13. Comparison of the values of $\bar{E}_0/R_{50}$ as a function of R_{50} calculated by EGS4 and ETRAN (Ref. 3) with the 1983 stopping powers (Ref. 19). The calculations are for broad parallel monoenergetic beams and R_{50} is the depth at which the absorbed dose to water falls to 50% of its maximum value. The AAPM protocol (Ref. 7) uses a constant value of 2.33 as an approximation of the ETRAN curve. The EGS4 curve can be reproduced within 0.4% by Eq. (2) in the text.

E_0. Secondly, note that the practical range R_p is not the same for the calculations with the full spectrum and the monoenergetic E_p spectrum, suggesting that R_p is not an ideal specification of E_p, as is commonly assumed.[8,9] In these cases, R_p varied by 1% (10 MeV) and 1.5% (20 MeV) for two spectra with the same value of E_p.

The third point to note is that using the realistic spectrum moves the calculated depth-dose curves towards the experimental data in two ways. With the realistic incident spectrum the surface dose is higher and the projected range is deeper than for the $\bar{E}_0$ spectrum. However, these improvements still do not explain all the differences, the causes of which remain unresolved.

In summary, the experimental data show a clear preference for the EGS calculations over the ETRAN calculations, as expected because of the errors in ETRAN associated with using the L(BL) energy-loss straggling distribution.

V. ENERGY SPECIFICATION OF ELECTRON BEAMS

Since the AAPM protocol's specification of the energy of electron beams is based on the Monte Carlo depth-dose curves calculated with ETRAN, the results presented above suggest that this procedure should be reexamined.

The procedure starts from the calculated ratio $\bar{E}_0/R_{50}$ as a function of R_{50}, where $\bar{E}_0$ is the incident energy for broad parallel beams of electrons incident on a water phantom and R_{50} is the depth at which the dose falls to 50% of its maximum value. Figure 13 compares the values calculated by EGS and by ETRAN. For example, a measured value of R_{50} = 8.5 cm would imply $\bar{E}_0$ = 20.1 MeV using the EGS values, but only 19.4 MeV using the ETRAN values (a difference of 3.6%).

For convenience, the AAPM protocol has approximated the ETRAN curve given in Fig. 13 with a constant value of 2.33, which actually reduces the magnitude of the discrepancy for energies between 10 and 36 MeV (or R_{50} from 4.3 to 15.9 cm). The AAPM protocol also ignores beam divergence effects. We have calculated these effects using a $[\mathrm{SSD}/(\mathrm{SSD}+Z)]^2$ correction to calculate depth-dose curves for a given source–surface distance (SSD) from the broad beam results and have extracted R_{50} from these curves. The results are summarized in Fig. 14 and Table III. Ignoring the SSD effect produces a 2.4% error in $\bar{E}_0$ at SSD = 100 cm for a 30-MeV electron beam and a 1% error at SSD = 80 cm for beams of 15 MeV. At an SSD of 100 cm, the combination of considering SSD effects and using the EGS4 results instead of the constant AAPM value implies increases in the calculated $\bar{E}_0$ varying from 2.6% at 20 MeV to 10% at 40 MeV and 15% at 50 MeV; or 4.2% at 10 MeV and 10% at 5 MeV. While we agree with Schulz and Meli,[34] TG-21 (1986),[35] and Wu *et al.*[36] that these considerations regarding $\bar{E}_0$ will not change the dose determination nearly as much as they change $\bar{E}_0$, problems seem to be inevitable with a protocol which assigns mean energies which are consistently low by 2.5% to 15%. We believe depth-dose curves should be corrected to an infinite SSD and the mean energy at the surface should be determined using the data in Fig. 14 to deduce the ratio $\bar{E}_0/R_{50}$ from the measured value of R_{50}. In the energy

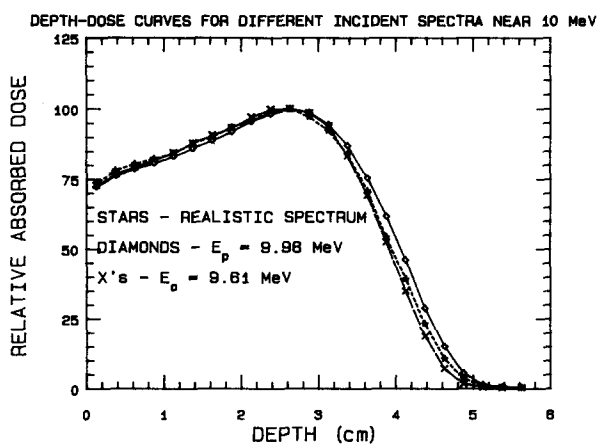

FIG. 12. Same as Fig. 11 except for the spectrum shown in Fig. 10.

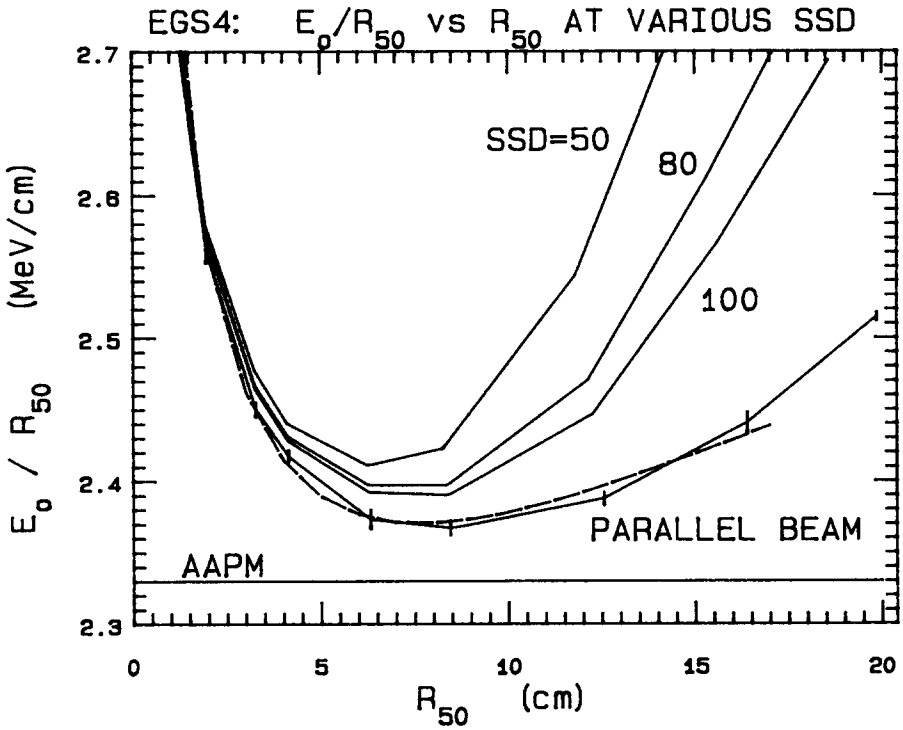

FIG. 14. Values calculated by EGS4 for $\overline{E}_0/R_{50}$ as a function of R_{50} for various values of SSD. The constant value recommended by the AAPM is also shown. The values for the parallel beam case predicted by Eq. (2) in the text are shown as a dashed line.

range from 5 to 40 MeV ($R_{50} = 2$ to 16.4 cm) the following formula reproduces the EGS broad parallel beam data to within 0.4%:

$$\overline{E}_0/R_{50} = 2.806 - 0.4288 \ln R_{50} + 0.1056(\ln R_{50})^2, \quad (2)$$

where $\overline{E}_0$ is in MeV and R_{50} is in cm.

In all of the above we have ignored the fact that the derivation is based on calculated depth-*dose* curves, but the AAPM protocol states R_{50} can be determined from depth-*ionization* curves. Wu *et al.*[36] have shown that using depth-ionization curves is incorrect, and on average, correcting to a depth-dose curve increases the beam energy by another 2%. Until we have a set of EGS calculated stopping-power ratios we cannot quantitatively determine the corrections needed for depth-ionization curves in a completely consistent manner. However, they should be very similar to those deduced by Wu *et al.*[36]

TABLE III. R_{50}, the depth in a water phantom at which the dose falls to 50% of its maximum value, as a function of beam energy and SSD. All values are based on broad parallel beam calculations done with EGS4 using the 1983 stopping powers.

$\overline{E}_0$ (MeV) SSD(cm):	R_{50}(cm) ∞	100	80	50
3	1.097(5)[a]	1.094	1.093	1.091
5	1.952(6)	1.945	1.944	1.939
8	3.265(7)	3.247	3.243	3.230
10	4.138(8)	4.119	4.114	4.098
15	6.320(16)	6.271	6.259	6.221
20	8.451(18)	8.370	8.345	8.255
30	12.56(3)	12.26	12.143	11.79
40	16.39(5)	15.59	15.31	14.65
50	19.88(2)	18.56	18.16	16.76

[a] Values in brackets are the one standard deviation uncertainties in the last digit. The same values apply to all SSD values on each line.

VI. CONCLUSIONS

We have shown that electron depth-dose curves in water calculated with ETRAN are systematically low near the surface because ETRAN uses the Blunck–Leisegang modification of the Landau energy-loss straggling formalism, which produces a mean energy loss which is low by about 10%. The surface dose calculated with EGS is higher because it uses the correct mean energy loss. We have shown that in water the multiple scattering formalisms in the two codes lead to very similar results if energy-loss straggling is ignored.

Experimental data are in better agreement with the depth-dose curves calculated by EGS, although there are still some minor discrepancies. Exploratory calculations taking into account energy straggling in the radiators, filter, and air indicate that neither $\overline{E}_0$ nor E_p are ideally specified by R_{50} and R_p, respectively. The effect of this energy straggling in the beam is, as expected,[37] to increase the relative surface dose somewhat and decrease the slope of the dose falloff region, making the calculations in better agreement with experiment.

We have presented a simple formula relating the most probable energy of an electron beam to the measured practical range for electron beams with energies between 3 and 50 MeV. Below 20 MeV this formula is in good agreement with the previous formulas based on ETRAN because the practical range is defined by electrons which do not undergo large energy-loss events and EGS and ETRAN produce similar results for these cases. Above 20 MeV the EGS results are lower than ETRAN results, reaching 6% less by 50 MeV.

We have presented detailed data relating $\overline{E}_0$, the mean energy of the electron beam, to R_{50}, the distance at which the dose reaches 50% of its maximum, including a simple formula which applies to the infinite SSD case for monoenergetic electron beams in the energy range $5 \leqslant \overline{E}_0 \leqslant 40$ MeV. The differences in the beam energy when calculated with the

AAPM protocol or using our new data and correcting for SSD amount to at least 2.6% (SSD = 100, $E = 20$ MeV) and go to over 10% for $E \geqslant 40$ MeV and $E \leqslant 5$ MeV. As shown elsewhere,[34–37] the changes in the final dose calculations due to changes in the specification of the energy of the beam are expected to be much smaller. Our results also imply that the actual stopping-power ratios as a function of depth may change because of the differences in the slowing down spectra calculated by EGS and ETRAN. Thus a completely consistent treatment awaits stopping-power ratios calculated using EGS, but the further changes are expected to be small.

ACKNOWLEDGMENTS

We wish to thank Stephen Seltzer of the NBS for many long, fruitful discussions about subtle differences between ETRAN and EGS, Pedro Andreo of the Zaragoza University Hospital for comments on the manuscript, and Alan Nahum of the Royal Marsden Hospital for comments on the manuscript and for pointing out the argument concerning the equality of the practical ranges.

[1]M. J. Berger, in *Methods in Computational Physics*, edited by B. Alder, S. Fernbach, and M. Rotenberg (Academic, New York, 1963), Vol. 1, pp. 135–215.
[2]S. M. Seltzer and M. J. Berger, in *National and International Standardization of radiation dosimetry, Proceedings of the Atlanta Symposium, 1977* (IAEA, Vienna, 1978), Vol. 2, pp. 3–43.
[3]M. J. Berger and S. M. Seltzer, Natl. Bur. Stand. (U.S.) Report No. NBSIR-82-2451, 1982.
[4]M. J. Berger and S. M. Seltzer, documentation for RSIC Computer Code Package CCC-107, ORNL, 1973.
[5]M. J. Berger and S. M. Seltzer, Phys. Rev. C **2**, 621 (1970).
[6]S. M. Seltzer and M. J. Berger, Nucl. Instrum. Methods **119**, 157 (1974).
[7]Task Group 21, Radiation Therapy Committee, AAPM, Med. Phys. **10**, 741 (1983).
[8]Nordic Association of Clinical Physics, Acta. Radiol. Oncol. Radiat. Phys. Biol. **19**, 55 (1980).
[9]International Commission on Radiation Units and Measurements Report No. 35, 1984.
[10]International Commission on Radiological Protection Report No. 21, 1971.
[11]R. L. Ford and W. R. Nelson, SLAC Report No. SLAC-210, 1978.
[12]W. R. Nelson, A. Hirayama, and D. W. O. Rogers, SLAC Report No. SLAC-265, 1985.
[13]D. W. O. Rogers, Health Phys. **46**, 891 (1984).
[14]J. A. Halbleib, Sr. and W. H. Vandevender, Nucl. Sci. Eng. **61**, 288 (1976).
[15]A. E. Nahum, Ph.D. thesis (University of Edinburgh, 1976).
[16]P. Andreo and A. Brahme, Radiat. Res. **100**, 16 (1984); and P. Andreo, in *The Computation of Dose Distributions in Electron Beam Radiotherapy*, edited by A. E. Nahum (Umea University, 1985), Chap. 6, p. 80.
[17]P. Andreo (private communication, 1984).
[18]M. J. Berger and S. M. Seltzer, NASA Report No. NASA SP-3012, 1964.
[19]M. J. Berger and S. M. Seltzer, Natl. Bur. Stand. (U.S.) Report No. NBSIR 82-2550-A, 2nd ed., 1983.
[20]R. M. Sternheimer, S. M. Seltzer, and M. J. Berger, Phys. Rev. B **26**, 6067 (1982).
[21]R. M. Sternheimer and R. F. Peierls, Phys. Rev. B **3**, 3681 (1971).
[22]D. W. van de Putte and D. J. Cusens, Phys. Lett. **51** A, 393 (1975).
[23]M. S. Weinhous and R. Nath, Med. Phys. **11**, 254 (1984).
[24]J. S. Findlay and A. R. Dusautoy, Nucl. Instrum. Methods **174**, 531 (1980).
[25]D. W. O. Rogers, Nucl. Instrum. Methods A **227**, 535 (1984).
[26]D. W. O. Rogers and A. F. Bielajew, Natl. Res. Counc. Can. Report No. PXNR-2692, 1984.
[27]H. M. Colbert, Sandia Laboratories Report No. SLL-74-0012, 1973.
[28]J. A. Halbleib, Sandia Laboratories Report No. SAND79-0415, 1979.
[29]J. A. Halbleib and T. A. Mehlhorn, Sandia Laboratories Report No. SAND84-0573, 1984.
[30]S. M. Seltzer (personal communication, 1985).
[31]I. Lax, A. Brahme, and P. Andreo, Acta Radiol. Suppl. **364**, 49 (1983).
[32]K. R. Shortt, C. K. Ross, A. F. Bielajew, and D. W. O. Rogers, Phys. Med. Biol. **31**, 235 (1986).
[33]C. K. Ross and K. R. Shortt, Natl. Res. Counc. Can. Report No. PIRS-0021, 1985.
[34]R. J. Schulz and J. A. Meli, Med. Phys. **11**, 872 (1984).
[35]R. J. Schulz, P. R. Almond, G. Kutcher, R. Loevinger, R. Nath, D. W. O. Rogers, N. Suntharalingam, K. A. Wright, and F. M. Khan, Med. Phys. **13**, 755 (1986).
[36]A. Wu, A. M. Kalend, R. D. Zwicker, and E. S. Sternick, Med. Phys. **11**, 871 (1984).
[37]P. Andreo and A. E. Nahum, Med. Biol. Eng. Comp. Suppl. 1 **23**, 608 (1985).
[38]M. Kotera, K. Murata, and K. Nagami, Phys. Status Solidi B **133**, 203 (1986).